Engineering Structures 181 (2019) 293–309

Contents lists available at ScienceDirect

Engineering Structures

journal homepage: www.elsevier.com/locate/engstruct

Curvature based DAD-method for damage localisation under consideration of measurement noise minimisation

Dolgion Erdenebat[a,*], Danièle Waldmann[a], Norman Teferle[b]

[a] University of Luxembourg, Institute for Civil Engineering and Environment, 6, Avenue de la Fonte, L-4364 Esch-sur-Alzette, Luxembourg
[b] University of Luxembourg, Institute for Civil Engineering and Environment, 6, rue Richard Coudenhove-Kalergi, L-1359, Luxembourg

A B S T R A C T

Several research projects on condition assessment of bridges have proven that structural responses from dynamic excitation or static loading are influenced by local damages and thus, could be used for the detection and localisation of damages. Particularly, the curvature of structures is directly depending on their stiffness. In order to localise the discontinuities in curvature lines resulting from damage, this paper uses the so-called Deformation Area Difference Method (DAD), which is based on static load deflection tests on bridge structures. The DAD-method for damage localisation is presented within the paper using a theoretical example, which is then verified by two laboratory experiments. The first experiment consists of a reinforced concrete beam, which is loaded stepwise until failure of the concrete in the compression zone. Due to the load increase, the tensile zone of the beam starts cracking, leading to a stiffness reduction. The application of the DAD-method allows identifying the cracked area from the measurement of the deflection line. However, a challenge and a prerequisite for the applicability of the DAD-method is the highly accurate measurement of the deflection line. Therefore, one of the most modern measurement techniques such as digital photogrammetry is applied. Nonetheless, the accuracy of each measurement technique is limited. The second laboratory experiment consists of a steel beam, which is locally damaged at three positions. The degree of the damage is stepwise increased in order to identify at which degree of damage the applied DAD-method is still able to identify and localise damage.

In this work, the focus lies on the minimisation of the effect of noise resulting from the limited measurement precision. Possible solutions were examined and proposed based on methods such as data smoothing using polynomial regression, consideration of standard deviation and measurement point variation. The reduction of the noise effect leads to an increase in the sensitivity of the damage localisation. The DAD-method has proven its potential for practical application through the successful localisation of cracking in the concrete beam.

1. Introduction

Over the past few decades, against the background of the rapid development of international transport, the maintenance, repair and preservation of infrastructure is becoming increasingly important. Structures such as bridges are core elements of a healthy infrastructure and ensure besides the crossing over the barriers, the secure traffic flow in the main hub of roads. In 1970, the proportion of road freight transport amounted to about 52,1% in the 15 EEC countries which reached 79,3% in 2002 [1]. According to the report on transport from the European Commission, the portion of freight transport will reach expectedly about 80% by 2050 [2]. The bridge structures and roads are claimed differently depending on the weight and transition of individual vehicles whereas not vehicles are relevant but the number and weight of the passing axles. In order to estimate the influence of the different axle transitions on the structure's condition, AASHTO-Road-Tests [3] has determined an equivalence factor to convert lighter or heavier axle loads to a standard 10 tons axle load. The reference value of the axle load amounts to 10 tons. This assumes that damage increases with the fourth power of the static axle loads. A 12 tons-truck with a front axle load of 5 tons and a rear axle load of 7 tons causes approximately 1/3 of the damage compared to a single passage of a standard 10 tons axle load (Eq. (1)). So, the comparison of a car with an axle load of 1 ton and a truck with an axle load of 10 tons clearly shows the impact of trucks on road or bridge structures. Namely, a car with axle load of 1 ton causes 1/5000 times less damage than a truck with an axle load of 10 tons (Eq. (2)) [4].

$$\left(\frac{5t}{10t}\right)^4 + \left(\frac{7t}{10t}\right)^4 = 0,30 \cong \frac{1}{3} \tag{1}$$

$$\left(\frac{1t}{10t}\right)^4 + \left(\frac{1t}{10t}\right)^4 = 0,002 = \frac{1}{5000} \tag{2}$$

Statistics show the number of bridges for several countries:, the USA counts over 600 000 interstate, state and city bridges and Germany counts about 35 000 road bridges and about 30 000 railway bridges [5]. About 11% of the bridges in the USA and about 12% of the bridges in Germany [6] have been identified as structurally deficient [7]. The

* Corresponding author.
E-mail addresses: dolgion.erdenebat@uni.lu (D. Erdenebat), daniele.waldmann@uni.lu (D. Waldmann), norman.teferle@uni.lu (N. Teferle).

https://doi.org/10.1016/j.engstruct.2018.12.017
Received 26 April 2018; Received in revised form 5 December 2018; Accepted 6 December 2018

increasing average age of the existing bridges shows a growing tendency for deficient structures. Each country has its own rules about the local onsite inspection sequence of existing bridges, which always requires considerable effort, skilled and trained staff and appropriate technique. These facts explain the urgent need for appropriate methods for reliable condition assessment of bridges.

Many studies have examined the damage levels of bridges and impacts, which are influencing the load bearing capacity of bridges [8,9] and confirm that damage leads to a change in the structural response of the structures by static loading tests as well as dynamic excitation tests [10]. This expertise is nowadays used by many research projects for developing long term monitoring concepts for structures. The long-term monitoring systems are used to control all changes in the structural response, which become apparent during the measurement period. The verification of possible changes in the structural response are detected by comparing the new data with initial measurement results as well as by comparing them with the results of a numerical model of the structure [11]. However, long term monitoring of structures comprises several problems. At first, structural health monitoring only allows to measure the structural response over its lifetime, but it cannot serve as independent method for condition assessment of bridge structures. The measured data is also difficult to be integrated into the bridge model. The newly installed measurement techniques for long-term monitoring are threatened by aging effects, because the ageing processes of those measurement techniques are usually faster than the aging of the structure itself. Some investigations [12] show that the effort of early failure warning systems by using real-time monitoring. However, such early warning systems cannot predict sudden failures such as, e.g., failures due to shear which always occur suddenly and brittle compared to a ductile failure due to bending [13,14]. Compared to methods based on mode shapes and traditional frequency analysis, methods based on static loading tests show several advantages. Lantsoght et al. [15] summarised the state-of-the-art on load testing of concrete bridges. Particularly, the diagnostic load testing, proof load testing, testing of other types of structures and current codes and guidelines were discussed. The authors argue that there is still a need for the development of a unified recommendation for proof load, loading protocol and stop criteria.

Static load deflection experiments with defined position of load or with moving load along the longitudinal axis of the structure provide clearer statement about damage assessment. Stöhr et al. [16] presents a method based on static measurements using a inclinometer applied to beam systems. The inclinometer is positioned at the support of the beam, which is stressed under a moving load. The aim of the study was to compare the initial measurement of the influence line with the one after the local stiffness reduction to enable the localisation of damage. Despite the noise of the inclination measurement, the influence lines from both damage scenarios show good tendency in agreement to the calculated FE-Model. The author showed also the possibility of positioning the inclinometer near mid-span. In the second half of the paper, an experiment on a real pedestrian bridge was presented. The 23,56 m long bridge was loaded with a truck with a total weight of about 6,0 tons. The total weight of the truck was equal to the applied uniform design live load, wherefore the test could be considered to be non-destructive. Due to this loading a stiffness reduction of 15% was achieved. Further comparable research projects using inclinometers and influence lines were presented in [17] and [18].

Sun et al. [19] developed a method based on the evaluation of curvature to detect damages in structures such as bridges. The main objective of their study was to minimize the noise effect of the measurement technique under consideration of the standard deviation. This paper showed results from a laboratory experiment with a steel beam and results from a finite element bridge model. The experimental beam was loaded at different positions along the beam. The measurement of the movement took place at mid-point using a laser displacement meter. The local damage, respectively, stiffness reduction of 60% was created at the one-third-way of the span. The length of curvature interval was investigated for several cases. Consequently, the minimum ratio of noise/damage effect could be calculated. Therefore, it is advised to minimize the noise level under consideration of the noise/damage ratio. For both cases, the laboratory experiment and the finite element calculation, the damage localisation was better traceable for a damage severity of over 50%.

He et al. [20] presented a damage detection method for beam structures using quasi-static moving load induced displacement responses. They investigated the correspondence between damage parameters and displacement influence lines. The theoretical background of the method is based on the features of the Euler-Bernoulli method [21]. The effectiveness of the proposed method was proven by using numerical and experimental examples. The change in the displacement influence line (DIL) indicated the damage, from which the damage localisation index could be deduced. The application of the method was subdivided as follows: first, the localization of the damage using the DIL, then the damage level quantification can take place. For the damage level quantification, a certain number of displacement sensors was needed, which should be positioned in the area of localized damage. The measured and calculated DIL showed peaks in the region of damage. However, the effect of noise resulting from the measurement affected the accuracy of damage localisation. Further corresponding damage detection methods using moving loads were presented in [22–25]

Technological developments have left their mark on measurement techniques. Modern measurement techniques such as digital photogrammetry opened new ways for the development of innovative methods for inspection of structures [26–28]. Close-range photogrammetry has already been used for the determination of the three-dimensional geometry of bridges since 1970 [29]. A literature review for the last 20 years is presented in [30]. Jiang et al. [31] used close-range photogrammetry for deflection measurement of a laboratory bridge test and of a field bridge test. The applied cameras for their study was a Kodak Pro SLR/n camera with a 36 × 24 mm, 13,85 million pixel CMOS sensor and a Kodak DCS660 camera with a 27x18 mm, 6 million pixel CCD sensor. The reached accuracy of the photogrammetric results for laboratory condition ranged from about −0,41 mm to +0,89 mm and for the field study from about +0,10 mm to +1,33 mm. Nishiyama, et al. [32] applied photogrammetric methods for crack monitoring. They used reflective targets around the crack in order to measure the change of the crack. The reached precision amounted to less than 0,10 mm using digital image captures from a distance of 10,0 m and less than 0,20 mm from a distance of 25 m. Comparable studies for the measurement with photogrammetric methods for laboratory or field tests were presented in [33,34]

The first part of the DAD-method was presented in [35] und included the theoretical background, several case studies with stiffness and temperature variations, as well as results from a laboratory experiment. In this work, the further development of the DAD-method is presented which considers the measurement precision, respectively, the standard deviation of the applied measurement technique. So, the measured deflection line could be smoothed in the range of the standard deviation in order to increase the precision of damage detection using the DAD-method. Since the smoothing of the curves requires a reference curve, a polynomial regression of multiple degrees was determined from the measured data. Riveiro et al. [33] described a similar process in their work, but they used the second degree of polynomial regression as the underclearance of bridges had been measured. Within the development of the DAD-method, in addition to the smoothing, several investigations have been carried out: various distances between the measurement points, automated evaluation process, correlation of several standard deviations due to measurement or hydraulic effects etc., have been analysed. The application has been verified by an additional laboratory experiment (Fig. 1), whereby the reduction of the noise effects becomes apparent due to the further development of the

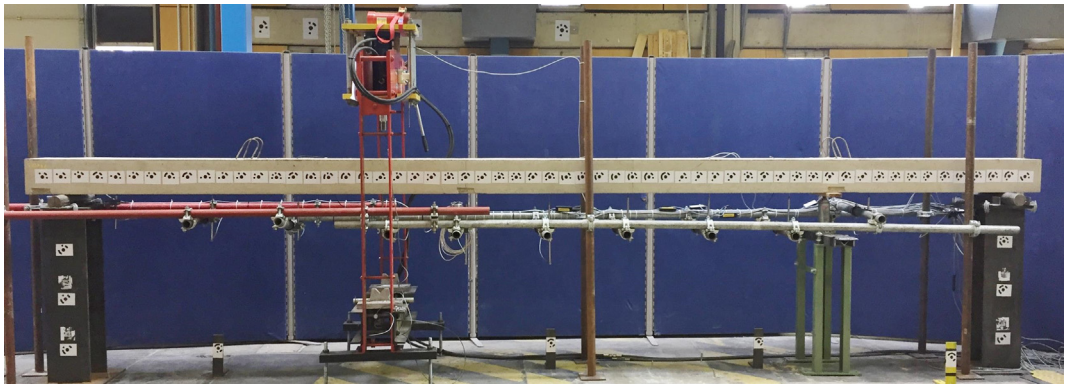

Fig. 1. Experimental reinforced concrete beam with eccentrical loading.

method.

Further laboratory experiments, theoretical applications of the DAD-method, and further comparisons of several modern measurement techniques were presented in [36–38]

2. The deformation area difference method (DAD-method)

The basis of the DAD-method is the bending line, respectively, the deflection line resulting from a theoretical model of a structure and from an in-situ load deflection measurement. In case of local structural damage, the continuous stiffness curve along the longitudinal axis will present a disruption. The stiffness of a structure is in relation to the bending moment and the curvature. The curvature corresponds, in case of small deflections, to the second derivation of the deflection line. The small deflection is ensured by the non-destructive load deflection test within the serviceability limit state. The first derivation of the deflection line corresponds to the inclination angle, whereby the second derivation of the deflection line corresponds, as already mentioned, to the curvature of the structure. In turn, the curvature is equal to the relation between the bending moment and stiffness of the structure [39,40]. Consequently, each stiffness change leads to discontinuities in the course of the curvature line. However, the change in stiffness can originate from possible damages, but also from the shape of the construction due to, e.g., coves, cross members or due to different widths over the length of the bridge. Therefore, the separation of both kinds of discontinuities is essential and a reference system including the scheduled stiffness change is required. A finite element model under consideration of the planned stiffness change along the longitudinal axis of the structure can be used as a reference system for the application of the DAD-method. Alternatively, an initial deflection measurement of a bridge structure can serve as a reference system after its manufacture. Subsequently, the discontinuity respectively the local damage of the structure will be localised using the algorithmic of the DAD-method.

The DAD-method considers particularly the area between the measured curves and the reference, respectively, theoretical curves of the deflection lines, inclination angles and curvatures from the load deflection experiment. In the following, the principle of the DAD-method will be introduced by using the results of the laboratory experiment (Fig. 1). The aim of the test is to localise the cracked area using the DAD-method based on a load deflection experiment. Fig. 2 shows exemplary the crack pattern in the beam for load step 20 kN. The cracks were detected during the experiment and illustrated in Fig. 2. The cracking in the reinforced concrete beam led to a stiffness reduction of approx. 60%.

The theoretical background will be presented using Fig. 2 and Fig. 3. The part a. of Fig. 3 illustrates the deflection lines $w_t(x)$ from the theoretical calculation serving as reference, $w_d(x)$ the deflection line with damage and $w_r(x)$ the deflection line from the polynomial regression. In a real application on a bridge the damaged deflection line $w_d(x)$ would be actually the measured deflection. To explain the method, the deflection line from the nonlinear calculation of the experimental beam was used in order to take into account the stiffness reduction caused by cracking. The polynomial regression is required to smooth the deflection line. A more detailed description and application of the polynomial regression can be found in Section 3.2. Part b. of the Fig. 3 shows the inclination angle from the reference system $\varphi_t(x)$, from the damaged system $\varphi_d(x)$ as well as from the polynomial regression $\varphi_r(x)$. Part c. shows the curvature for all three variants. The comparison of the stiffnesses between the linear calculation $EI_t(x)$ and non-linear calculation $EI_d(x)$ is illustrated in part d. of Fig. 3. The DAD-method particularly investigates the area between the reference curves and the measured curves, which is shown as blue area in Fig. 3. The considered area between the curves is then subdivided into several sections. The length of the sections corresponds to the distances between the deflection measurement points. The denser these points, the more accurate the localisation of the damage will be. Also, the mesh density of the finite element model of the structure must be at least as large as the distances of the measurement points. Subsequently, the individual areas are squared and normalized by the sum of the individual squares of the areas according to Eq. (3).

$w_t(x)$: Function of the theoretical deflection line

$w_d(x)$: Function of the measured resp. damaged deflection line

$w_r(x)$: Function of the polynomial regression of deflection

$\varphi_t(x)$: Theoretical inclination angle resulting from the first derivation of the theoretical deflection

$\varphi_d(x)$: Damaged inclination angle resulting from the first derivation of the damaged deflection

$\varphi_r(x)$: Function of the polynomial regression for inclination angle

$\kappa_t(x)$: Theoretical curvature resulting from the second derivation of the theoretical deflection

$\kappa_d(x)$: Damaged curvature resulting from the second derivation of the damaged deflection

$\kappa_r(x)$: Function of the polynomial regression for the curvature

The DAD-values are determined as already mentioned by the ratio between the squared area section and the sum of the squared area sections. The general formulation of the DAD-method is described in Eq. (3). The area differences between the theoretical and the measured results correspond to the difference between the integral functions of the theoretical and the measured characteristic equations regarding the deflection line, inclination angle and the curvature (Eq. (3)).

$$DAD_i(x) = \frac{\left[\int_{i-1}^{i} f_{d,i}(x)dx - \int_{i-1}^{i} f_{t,i}(x)dx\right]^2}{\sum_{i=1}^{n}\left[\int_{i-1}^{i} f_{d,i}(x)dx - \int_{i-1}^{i} f_{t,i}(x)dx\right]^2} = \frac{\Delta A_i^2}{\sum_{i=1}^{n}\Delta A_i^2} \quad (3)$$

$f_t(x)$: Theoretical function of the deflection line, the inclination

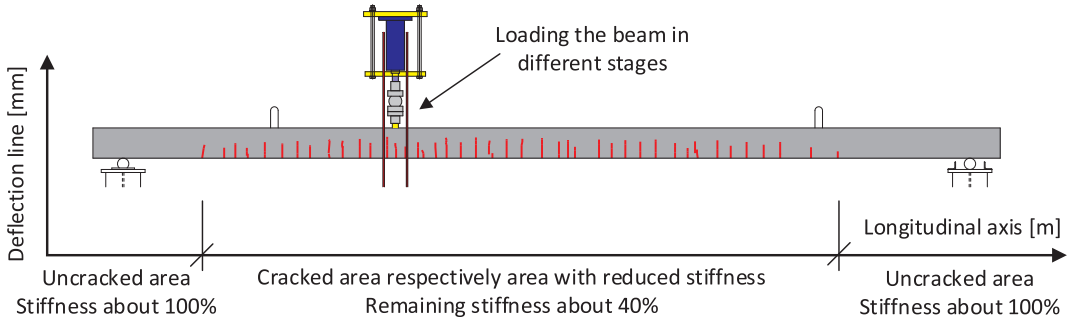

Fig. 2. Crack pattern of the experimental beam for load step 20 kN.

angle or the curvature

$f_d(x)$: Measured resp. damaged function of the deflection line, the inclination angle or the curvature

Consequently, it is possible to complete the common equation for the DAD-values (Eq. (3)) with each area difference value for deflection line (Eq. (4)), for inclination angle (Eq. (5)) and for curvature (Eq. (6)).

$$DAD_{w,i}(x) = \frac{\Delta A_{w,i}^2}{\sum_{i=1}^{n} \Delta A_{w,i}^2} = \frac{[w_d(x_i) - w_t(x_i) - w_t(x_{i-1}) + w_d(x_{i-1})]^2}{\sum_{i=1}^{n} [w_d(x_i) - w_t(x_i) - w_t(x_{i-1}) + w_d(x_{i-1})]^2} \quad (4)$$

$$DAD_{\varphi,i}(x) = \frac{\Delta A_{\varphi,i}^2}{\sum_{i=1}^{n} \Delta A_{\varphi,i}^2} = \frac{[w_d(x_i) - w_d(x_{i-1}) - w_t(x_i) + w_t(x_{i-1})]^2}{\sum_{i=1}^{n} [w_d(x_i) - w_d(x_{i-1}) - w_t(x_i) + w_t(x_{i-1})]^2} \quad (5)$$

$$DAD_{\kappa,i}(x) = \frac{\Delta A_{\kappa,i}^2}{\sum_{i=1}^{n} \Delta A_{\kappa,i}^2} = \frac{[\varphi_d(x_i) - \varphi_d(x_{i-1}) - \varphi_t(x_i) + \varphi_t(x_{i-1})]^2}{\sum_{i=1}^{n} [\varphi_d(x_i) - \varphi_d(x_{i-1}) - \varphi_t(x_i) + \varphi_t(x_{i-1})]^2} \quad (6)$$

Detailed descriptions, a derivation of the formula as well as several case studies are published in [35]. The application of the DAD-method based on a laboratory experiment, a consideration of measurement noise minimisation and the results will be presented in the following chapters.

3. Procedure of the DAD-method

The application of the DAD-method is summarized in the flowchart in Fig. 10. As already discussed, the the DAD-method is based on the measurement of the deflection line which is compared to a theoretical model of the investigated structure. The method is able to localise damages independent on the global influences such as temperature or non-structural layers such as the asphalt layer. However, the limitation of the damage detection depends on the precision of the applied measurement technique. Important prerequisites regarding the measurement techniques consist in a high density of measurement points to enable the creation of a continuous deflection line, high precision of the measurements and suitable applicability for in-situ bridge tests. The identification of discontinuities of the structure using the DAD-method is based on probability calculations considering the standard deviation of the applied measurement technique. According to the DAD-method, the deflection line is derived several times, in order to calculate the

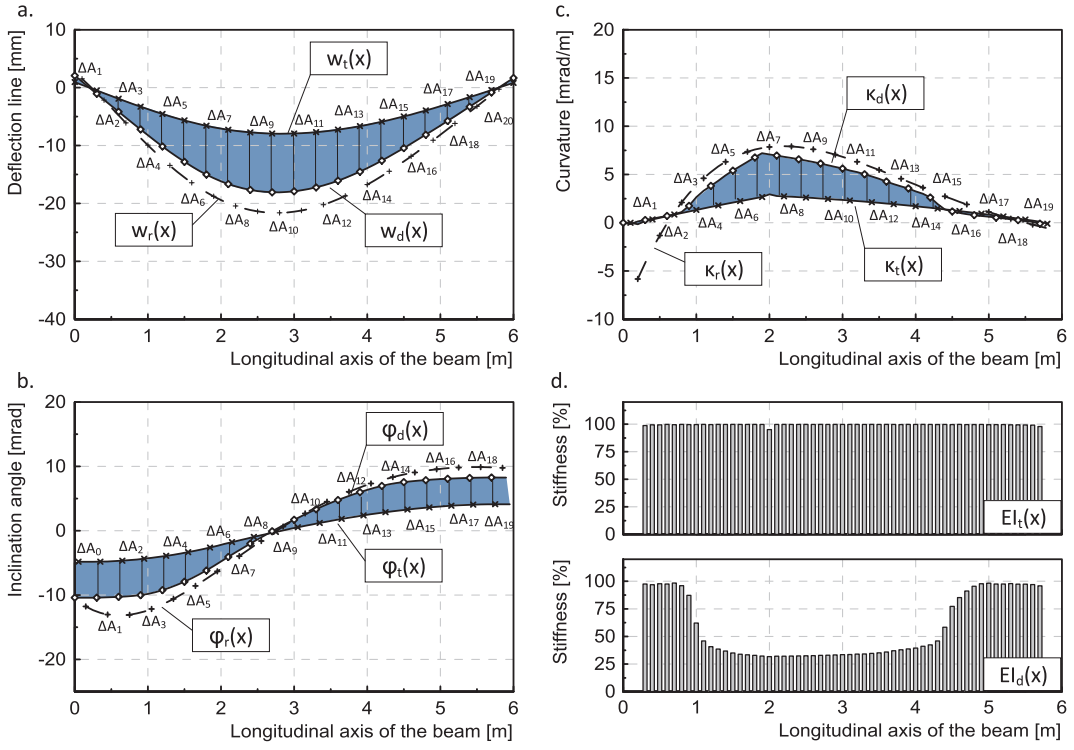

Fig. 3. Principle of the DAD-method illustrated by the laboratory experiment.

inclination angle and the curvature. Thus, the effect of noise resulting from the measurement precision increases obviously. The main advancement of the method compared to [35] is that the noise from the measurement is taken into account in the evaluation process. Although, the measurement with photogrammetric methods allows very high precision, but this is not absolute and has a certain standard deviation such as any other measurement technique. Therefore, the measured deflection line has a certain noise in the range of the standard deviation. Damage that causes discontinuities in the range of standard deviation cannot be clearly assessed. Therefore, in the next step, the measured deflection will be smoothed in the range of the standard deviation of the measurement technique so that only the discontinuities beyond the standard deviation become relevant.

The smoothing of the measured deflection requires a reference curve. Therefore, a polynomial regression of the measured deflection values was chosen as reference curve. A similar procedure was applied in the work of Sun, et al. [19]. Nonetheless, the degree of the polynomial regression should be chosen individually from one case to another, as it depends essentially on the type of the static system, the way of the loading and the shape of the deflection line. Riveiro et al. [33] used linear data fitting in their work because they measured the underclearance of bridge structures which usually has a straight course (a. Fig. 4). The laboratory experiment within this paper is stressed due to self-weight as well as due to a single load. The deflection curve resulting by a uniformly distributed load has the form of a fourth degree parabola whereas the deflection curve resulting from the single load has the form of a third degree parabola. Fig. 4 illustrates schematically the various possibilities for data fitting.

In the process of data evaluation, the decision on the degree of the polynomial regression is taken on the basis of the measured deflection line. The deviating values from the continuous course of the deflection line are shifted towards the direction of the polynomial regression within the range of the standard deviation of the measurement technique. Subsequently, the inclination angle and curvature will be calculated from the smoothed deflection values. In the next step, an additional consideration of measurement point variation will be taken into account. The individual steps of the procedure will be explained in more detail in the following subsections.

3.1. Standard deviation

The precision of the measurement of the deflection over the total length of a structure is limited by the scatter of the measurement technique. Each measurement technique has a limited precision; however most modern measurement techniques allow high accuracy and small standard deviations. The measurement of the deflection over the total length of the bridge structure comprises many data points, which form a point cloud. Each measured data point has an individual standard deviation. The deflection line of the experiment is measured by close-range photogrammetry. The photogrammetry is applied using a full-frame camera Nikon D800 and the point cloud is managed using a processing software of Elcovision 10. In order to allow high precision measurements, several settings and prerequisites must be taken into account. The camera is equipped with a 50 mm fixed focal length lens. An important prerequisite for precise measurement with photogrammetry is the calibration of the applied camera. For the calibration of the camera, the University of Luxembourg is equipped with a wall with a dimension of 13 × 7 m and with 163 photogrammetry targets (Fig. 5). The adjusted shutter speed amounts to 1/30 sec, ISO2000 and the F-stop amounts to f/10 and remains the same both for the calibrations and for the measurement of the specimen's deflection. The captures are taken using a remote camera shutter and from a tripod to avoid blurring.

The application of close-range photogrammetry allows high precision measurement of the deflection line, whereby the standard deviation of the technique is taken into account to reduce the noise effects and to smooth the measured deflection curve. Fig. 6 shows the standard deviations of each measurement point exemplary for the load steps 5 kN, 15 kN and 40 kN. The reached precision of photogrammetry varies in the range of 0,06 mm to 0,11 mm (Fig. 6).

3.2. Polynomial regression and smoothing of the deflection line

The calculation of the curvature leads to an increase of the noise effect due to double derivation of the measured deflection. Within the DAD-method, the discontinuity of the structural behaviour from a load deflection experiment is investigated. The DAD method has already demonstrated that even a very small stiffness change of 1% is identifiable when applying the method on deformation values from FE calculations [35]. So, the identification of damage will not be limited by the DAD-method itself, but only by the applied measurement technique. The accuracy of the measurement results by using photogrammetry is defined by the standard deviation with a probability of 66,7%. The experiment shows that the very accurate measurement of the photogrammetry achieves a minimum standard deviation of about 0,08 mm (Fig. 6), which could be improved depending on the camera and calibration quality. Discontinuities within the standard deviation cannot be separated from the measurement accuracy. However, it is possible to smooth the measured deflection data to identify discontinuities outside the standard deviation range. The identified discontinuities outside of the standard deviation point to stiffness changes respectively to damages. Damage producing discontinuities in the range of the standard deviation will not become apparent, but repeated measurements can minimize the probability of random peaks and will improve reliably the damage detection. The DAD-method is able to localize damage depending on the accuracy of the applied measurement technique: only

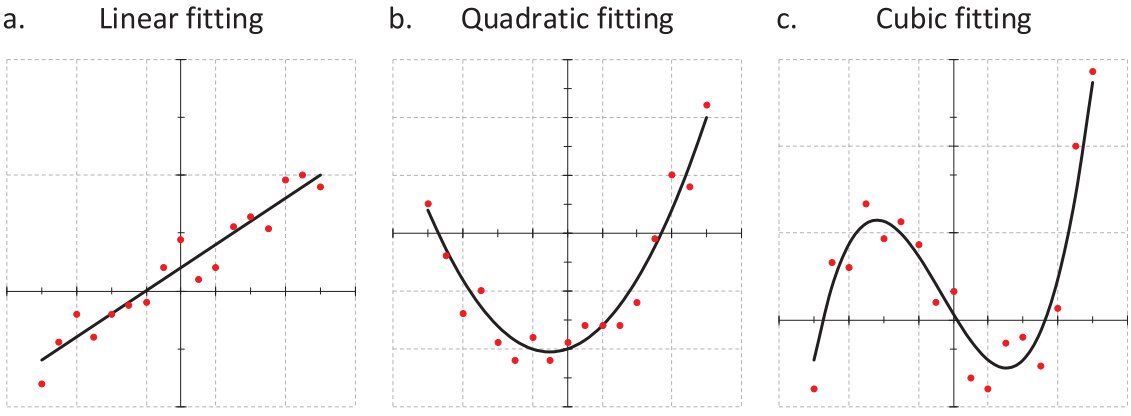

Fig. 4. Fitting of measured data a. linear fitting b. quadratic fitting c. cubic fitting.

Fig. 5. Process of camera calibration using a large scale calibration wall with the dimension of about 13,0 × 7,0 m and 163 targets.

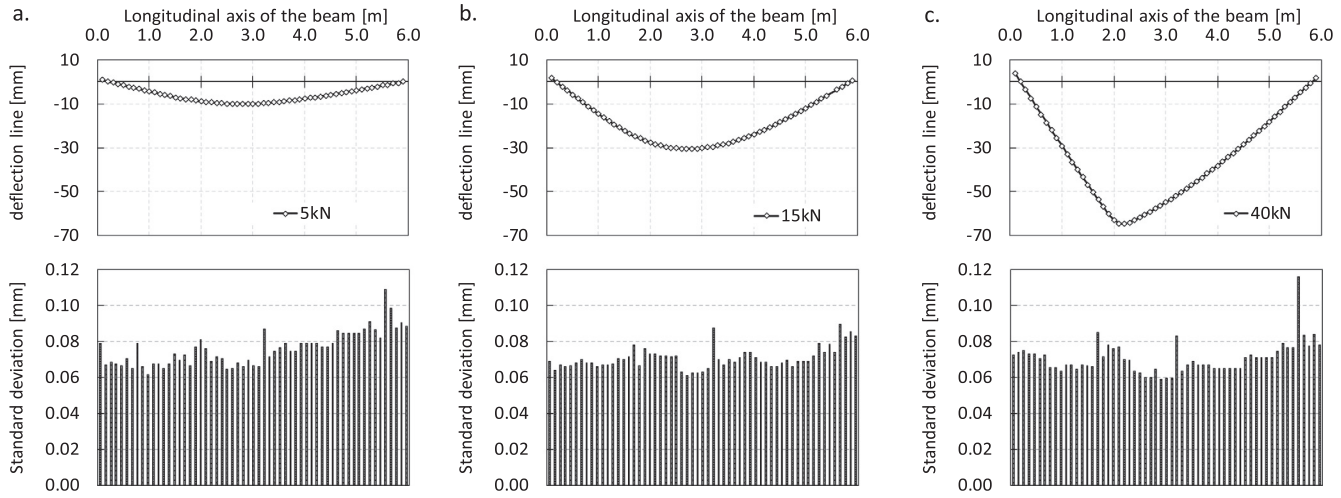

Fig. 6. Standard deviations resulting from close-range photogrammetry exemplary for the load steps 5 kN, 15 kN and 40 kN.

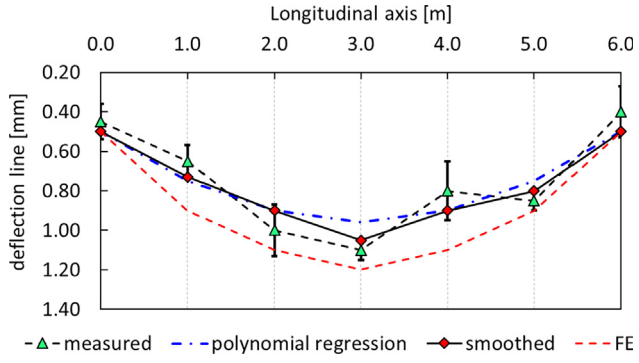

Fig. 7. Individual standard deviations for each measurement point.

damage, which affects the deflection measurements of a structure stronger as the variations inherent to the measurement accuracy, will become apparent. To illustrate this point, further investigations on the relationship between the measurement accuracy and the degree of damage is presented using the results of a second laboratory experiment in Section 4.5. In order to smooth the measured data, a reference curve is required. Fig. 7 shows the principle of the smoothing process. In Fig. 7, there are 7 measuring points in total (green triangular markers) for the deflection of a beam with 6 m span length. Each point has an individual standard deviation. The red dashed line shows the course of the deflection line from the FE calculation. A polynomial regression is generated from the measurement data and serves as reference curve for smoothing. The polynomial regression is shown in Fig. 7 with a blue dot-dash line. As already mentioned, the degree of the polynomial regression has to be chosen under consideration of the static system, type of loading and the form of the deflection line (Eq. (7)). The decision about the degree of polynomial regression has to be taken individually from case to case. A first verification of the regression degree can be done by comparing the second derivation of the measured deflection line with the polynomial regression line. The regression degree is augmented until these two lines show visually good agreement. However, the correspondence of the polynomial regression can also be expressed in numbers by using the correlation coefficient according to Pearson (Eq. (9)). The higher the degree, the closer the correlation to

the measured curve of deflection line.

Due to the precision of the measurements, the standard deviation resp. the noise is very small. Thus, the agreement in numbers according to Pearson is almost 100%. For the experimental beam a polynomial regression of the sixth degree is applied. The degree of the polynomial regression is chosen according to the agreement with the measured values. With this choice, the correlation coefficient amounts to 0,99 for all load levels. By smoothing the measured raw data, the measurement points are shifted within the range of the standard deviation in direction of the reference curve (Eq. (10)). Here, the reason why the polynomial regression is chosen as reference to smooth the measured value becomes clearer. If the deflection curve from the FE-calculation (red dashed line) would be used as reference curve to smooth the measured values, which are affected by noise (green triangular targets in Fig. 7), all measured values would be shifted together in the direction of the curve from FE due to smoothing process. In fact the measured values will be shifted only globally in direction of the reference and the effect of noise would remain the same. In contrast, when the reference curve is determined due to polynomial regression as an optimal continuous curve, the curve from the measured values is moved in the direction of the continuous reference curve. In other words, all measuring points are shifted individually in the direction of the continuous reference curve. The limit is, as already mentioned, the level of the standard deviation of the photogrammetry. In Fig. 7, the red rhombic markers represent the deflection points after the smoothing. Thus, the deflection line (solid black line) is created with less noise effect. By means of this smoothing process, the damage respectively the discontinuity can be identified separately from the measurable accuracies. Thus, any discontinuities that might be caused by the standard deviation of the measurement technique are excluded. Consequently, one has also to mention that all damage, which affects the structure in the range of the measurement accuracy, will remain undetected.

$$\begin{bmatrix} y_1 \\ y_2 \\ y_3 \\ \vdots \\ y_n \end{bmatrix} = \begin{bmatrix} 1 & x_1 & x_1^2 & \cdots & x_1^m \\ 1 & x_2 & x_2^2 & \cdots & x_2^m \\ 1 & x_3 & x_3^2 & \cdots & x_3^m \\ \vdots & \vdots & \vdots & \vdots & \\ 1 & x_n & x_n^2 & \cdots & x_n^m \end{bmatrix} \begin{bmatrix} a_0 \\ a_1 \\ a_2 \\ \vdots \\ a_m \end{bmatrix} + \begin{bmatrix} \varepsilon_1 \\ \varepsilon_2 \\ \varepsilon_3 \\ \vdots \\ \varepsilon_n \end{bmatrix} \tag{7}$$

$$\Rightarrow w_r(x) = \sum_{i=1}^{n} a_i x^i$$

$$r = \frac{\sum (x - \bar{x})(y - \bar{y})}{\sqrt{\sum (x - \bar{x})^2 \sum (y - \bar{y})^2}} \tag{9}$$

$$\begin{cases} w_d(x) = w_m(x) - 0,\ 50 \bullet s(x) \geq w_r(x), & if\ w_m(x) \geq w_r(x) \\ w_d(x) = w_m(x) + 0,\ 50 \bullet s(x) \leq w_r(x), & if\ w_m(x) < w_r(x) \end{cases} \tag{10}$$

y_i: Representation of the polynomial regression in the form of a matrix

$w_r(x)$: Function of the polynomial regression of deflection

r: Correlation coefficient according to Pearson

$w_m(x)$: Function of the raw measured deflection line

$w_d(x)$: Function of the measured resp. damaged deflection line after smoothing

s(x): Standard deviation resulting from the measurement technique

3.3. Consideration of measurement point variations

The density of the measurement points is of essential importance. In principle, the denser these points the more accurate will be the localisation of the damage. Nonetheless, the closer the points to each other, the smaller are the height differences between the points (Fig. 9). Fig. 9 also shows the standard deviations for the points. If the inclination angle will be determined from one point to the next point, the height differences between the points would be comparatively small (part a. Fig. 9) compared to the size of the standard deviation. Therefore, the results would be influenced more by the standard deviation. In comparison, in part b. of Fig. 9 a variation is given where only every third point is considered. There it can be seen that the standard deviation of the measurements was less influence on the results. The optimum ratio of the point distances depends on the standard deviation respectively on the size of the measurement noise, the size of the deflection and on the degree of damage. Sun et al. [19] represented the optimal relation between the noise, damage and curvature calculation interval, which has initially a decreasing tendency and then an increasing one. The optimal value is defined at the lowest point of the relationship (Fig. 8).

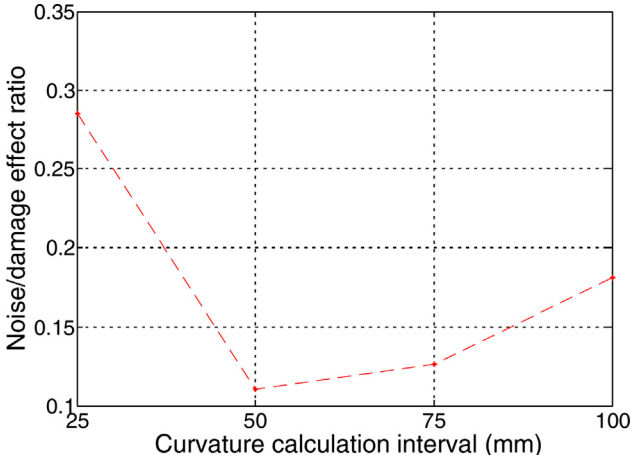

Fig. 8. Curvature calculation interval according to Sun et al. [19]

So, the precision of the damage localisation is depended on the measurement point distances. The application of this consideration becomes clearer using the results from the laboratory experiment in Section 4.3.

3.4. Summary of the evaluation procedure based on flowchart

In the following, the summary of the complete evaluation procedure will be presented using the flowchart in Fig. 10. The initial aim of the DAD-method is the detection and localisation of damage in bridge structures. The basics for the application of the method are on the one hand the theoretical model of the bridge structure considering all planned stiffness changes or the initial deflection measurement after the construction, and on the other hand the measurement of the deflection line. The prerequisite is in particular a high-precision measurement of the deflection line along the longitudinal axis of the bridge structure. Since the theoretical results from the finite element model are not affected by measurement noise, the inclination angle and the curvature of the reference curve can be directly determined. However, the measured deflection line includes an effect of noise due to measurement precision. As already mentioned, the smoothing of the measurement noise requires a reference curve, which is given by polynomial regression (part A. in Fig. 10). The degree of the polynomial regression should be calculated individually depending on the loading, deflection line and measurement noise. The smoothing of the raw data is presented in part B. of Fig. 10 and limited within the range of the standard deviation from photogrammetry. Several variations of the limit value analysis become necessary and will be calculated according to the Eq. (10). After the smoothing the deflection line, the inclination angle and the curvature are determined according to Eqs. (11) and (12) (part C. Fig. 10).

$$\varphi(x) = w'(x) = \frac{\delta w(x)}{\delta(x)} \tag{11}$$

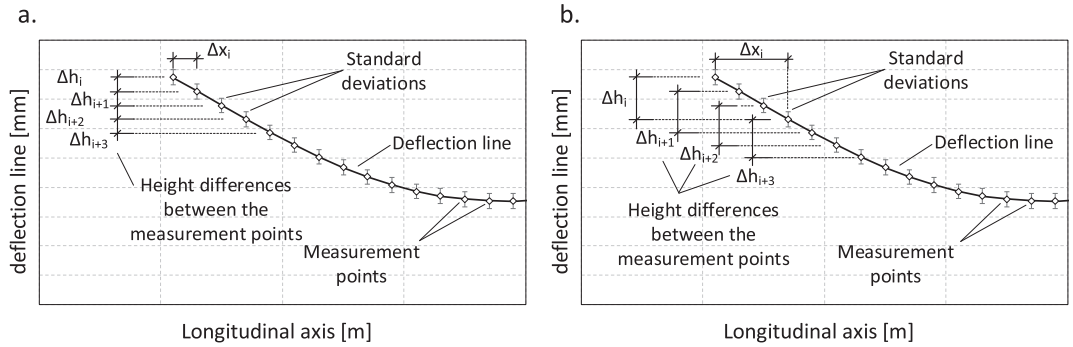

Fig. 9. Measurement point variations a. point to the next point; b. point to the next third point.

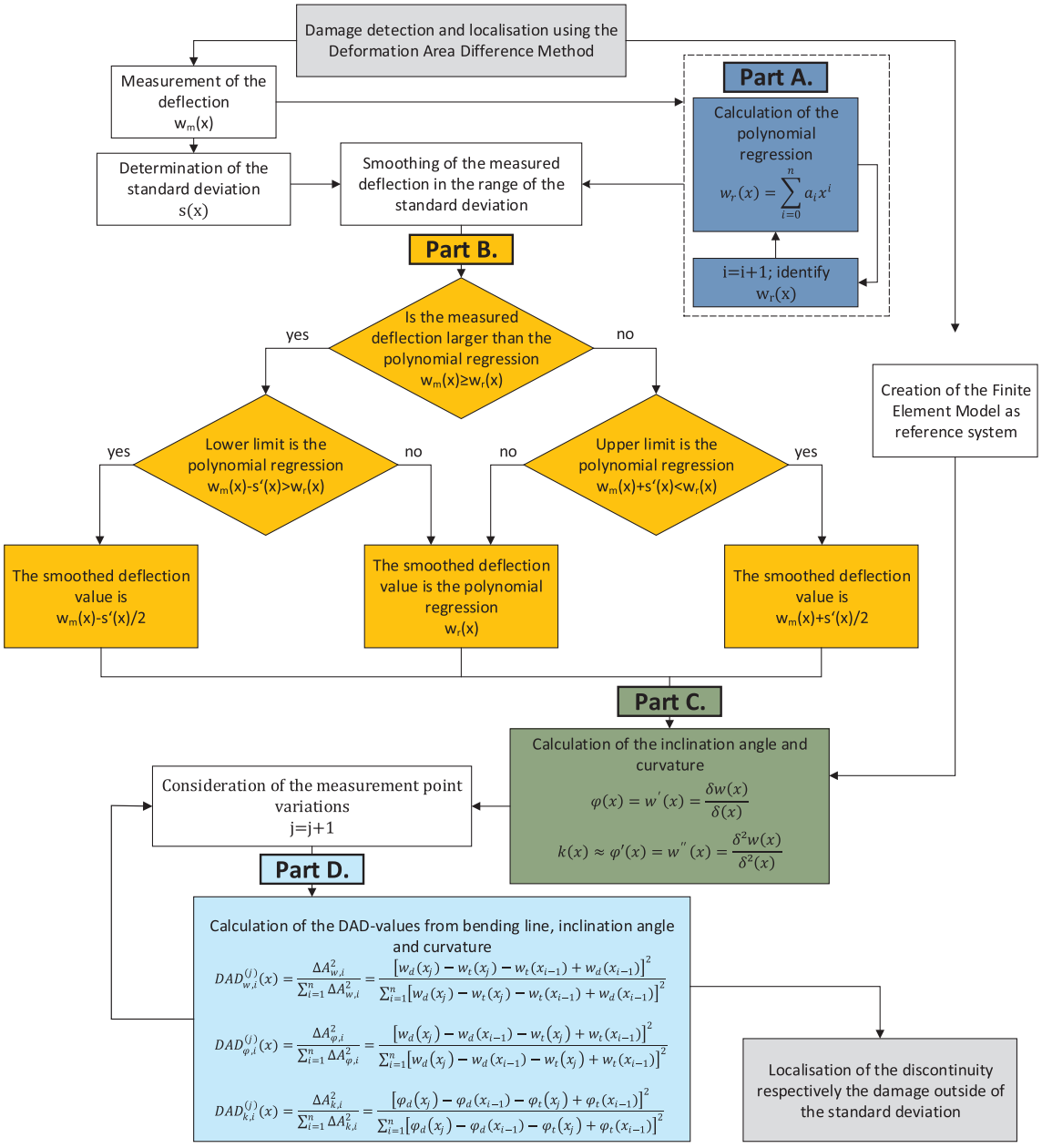

Fig. 10. Flowchart of the damage detection using the DAD-method.

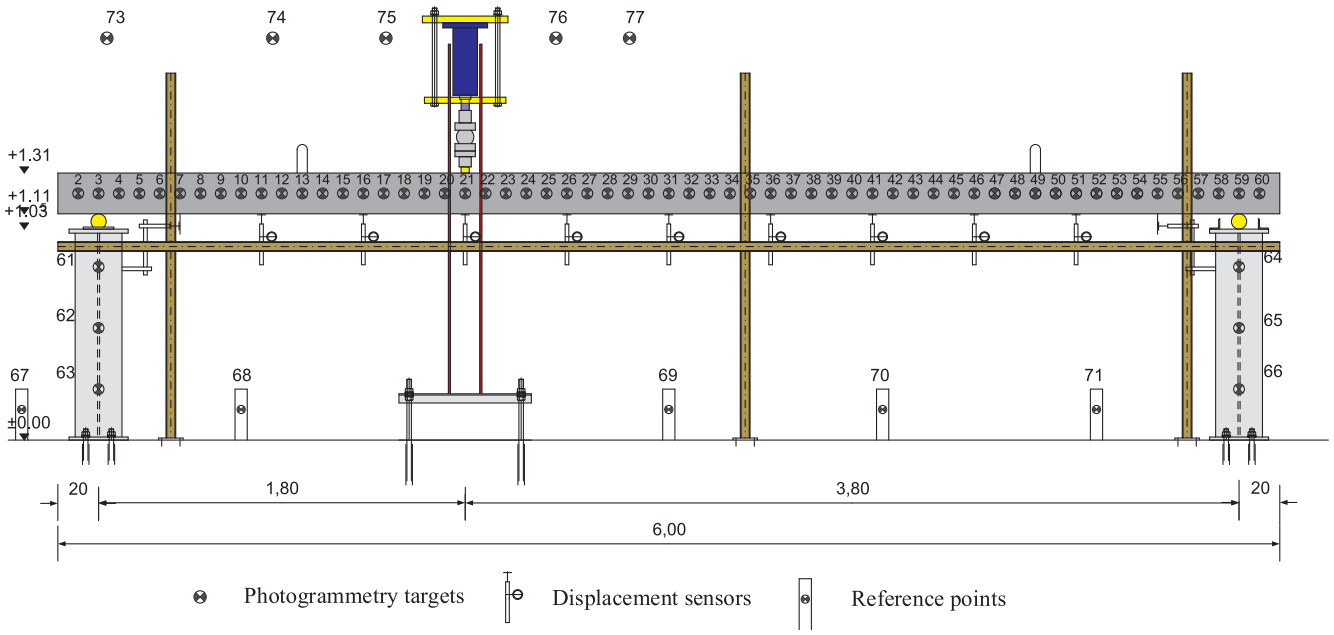

Fig. 11. Setup of the laboratory experiment with a reinforced concrete beam [38]

$$k(x) \approx \varphi'(x) = w''(x) = \frac{\delta^2 w(x)}{\delta^2(x)} \tag{12}$$

κ(x): Curvature
w(x): Bending resp. deflection
φ(x): Inclination angle

In the next step, as already explained in detail, the measurement point variation will be investigated. The aim of the measuring point variation is to find the optimum of measurement point distances from one measurement point to the next one. Finally, the algorithm of the DAD-method will be applied (Eqs. (4), (5), (6) and part D. of Fig. 10), whereby the peaks in the course of DAD-values indicate possible stiffness changes or damages.

4. Laboratory experiment

The application of the DAD-method for localization of damage, respectively, stiffness reduction is tested on an experimental beam (Fig. 11). The laboratory test consists of a reinforced concrete (Fig. 12) beam with a total length of 6,00 m and with a span of 5,60 m. The loading of the beam takes place eccentrically at 1,80 m from the left support. The loading is path-controlled and the load steps are 5 kN, 10 kN, 20 kN, 30 kN and 40 kN. At the first load step, the beam starts to receive cracks in the area of the load application. However, the first two load steps do not lead to excess of the deflection in the serviceability limit state. With the increasing load, the cracked area spreads along the longitudinal axis of the beam. The stiffness reduction resulting from cracking amounts about 60% for the experimental beam. In case of suitable localisation of the cracked area within the load steps 5 kN and 10 kN, the method could be suitable for its application within the serviceability limit state as non-destructive damage detection method. At the load step of 40 kN, the expected collapse of the beam occurred due to the concrete failure in the compression zone. The detection of each crack is accurately carried out with a crack magnifier. For each load step, the deflection line is measured using photogrammetry and displacement sensors. Along the beam, several coded photogrammetry targets were positioned at intervals of 10 cm. Reference targets were installed at the bottom, on both supports and in the background of the experimental beam (Fig. 11). The main objective of the experiment is to identify the discontinuities resulting from the different stiffness reduction scenarios and to compare them with the detected crack pattern.

4.1. Theoretical calculation compared to the measurement

Before the experimental test is carried out, the load deflection behaviour of the reinforced beam is investigated using linear and nonlinear calculation with the finite element software SOFiSTiK The statically determined single-span beam is simulated using the quad-elements with the side length of 10 cm. In order to create a model close to

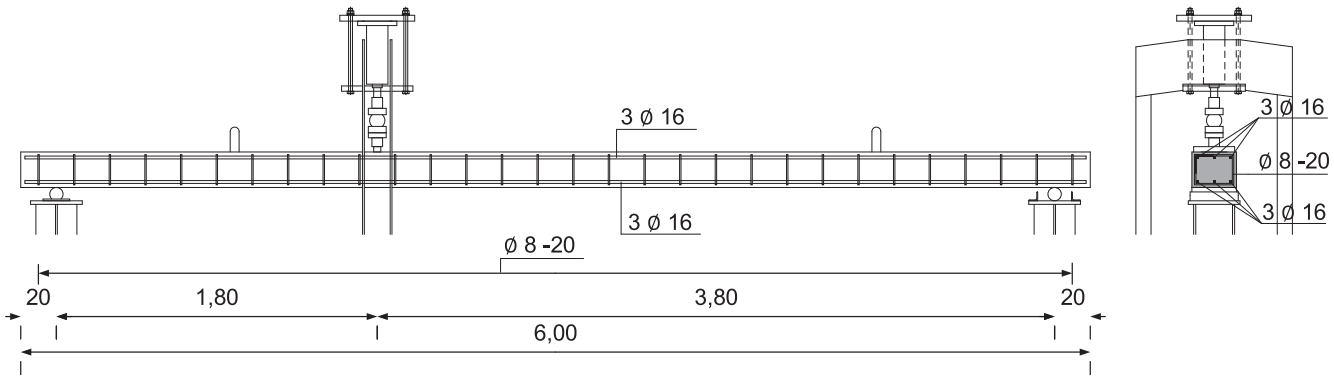

Fig. 12. Side view (left side) and cross sectional view of the loading situation and the laboratory beam (with reinforcement).

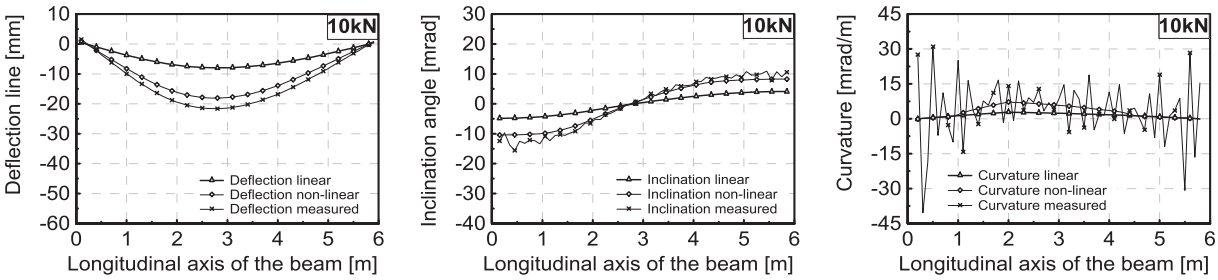

Fig. 13. Measured and calculated deflection lines, inclination angle and curvature for the load step 10 kN.

reality, the partial safety factors are set to 1.0 and the beam is stressed by a line load over the beam width. The non-linear calculation considers the stiffness reduction due to cracking, due to yielding of the reinforcement and concrete compression failure. Fig. 13, Fig. 14 and Fig. 15 show the deflection lines, inclination angles and curvatures for the load steps 10 kN, 20 kN and 40 kN. In Fig. 13, Fig. 14, it can be observed that the measured deflection is slightly larger than the deflection from the nonlinear calculation. Within the laboratory test, the reinforced concrete beam is loaded by path-controlled hydraulic. The stepwise loading of the beam took place by repeated loading and unloading, while the deflection due to creep effects increased continuously. For each load step took 2 h were needed to complete the measurement. Therefore, the difference between the measured and the calculated deflection can be explained by the additional creep deflections due to the stepwise loading and unloading process. Fig. 15 includes also the deformation values after concrete failure in the compression zone. Here, the deflection resulting from the nonlinear calculation is higher than from the measurement. This can be explained by the fact that the measurement of the deflection took place after unloading the beam where the elastic part of the deformation had already receded. As already mentioned, the inclination angle is calculated due to the first derivation of the deflection curve and the curvature due to the double derivation of the deflection line. The increased noise effect due to the multiple derivations is clearly recognizable in the following figures.

4.2. Consideration of the measurement accuracy and smoothing the curves

The standard deviation from the photogrammetric measurement ranges from 0,06 mm to 0,10 mm. The values of the standard deviation are used for the smoothing of the deflection curve according to the description of the DAD-method. As already discussed, in order to enable the smoothing of the deflection curve a reference curve is needed. Therefore, a polynomial regression is chosen as a reference system. The degree of the polynomial regression amounts to six for the experimental beam (for more information see Section 3.2). Fig. 16 and Fig. 17 show the curvature curves calculated from the second derivation of the measured deflection line for each load step as well as the polynomial regression sixth degree and the smoothed curvature course. It is important to choose the appropriate degree of the polynomial regression. Otherwise, the smoothing of the curve can have only a global effect without reducing noise the effects (see Section 3.2). The second derivation of the polynomial regression is the curvature of the polynomial regression, which is presented as red line in Fig. 16 and in Fig. 17. The tendency of the curvature line resulting from the polynomial regression shows some deviations at the beginning and at the end of the longitudinal axis of the beam. This is particularly visible in part c. of Fig. 16 and in Fig. 17. Here, the polynomial regression is not at the average of the curvature noise. The consequences thereof become clear in the experimental result related to the following chapter.

4.3. Consideration of measurement point variations

An important aspect of the data evaluation is the considered section length. Indeed, the distance between the measurement points respectively the density of the point cloud will directly influence the damage localisation accuracy. However, the considered section length must be chosen such that the noise effects of the measurement technique have limited influence only. For the laboratory experiment, the density of the measurement point amounted to 10 cm. Due to small deflections at the lower load steps, the resulting deflections remain small. Consequently, the height differences between one point to the next point is with a distance of 10 cm very small so that the standard deviation generates too much noise. Fig. 18 shows the influence of the measurement point distance Δx_i variation depending on the noise s(x) and height difference Δh_i relation. In order to represent the ratio in percent, the influence of the standard deviation $(s(x)/\Delta h_i)$ for the case $\Delta x_i = 10$ cm is set to 100% (Fig. 18). The standard deviation from the measurement technique behaves relatively constant as shown in Fig. 6. Fig. 18 clearly showed that the influence of the standard deviation for smaller height differences (see also Fig. 9) is considerably bigger and decreases exponentially as a function of the measurement point distances Δx_i. Fig. 19 shows the DAD-values for four investigated variations of possible section lengths (10 cm, 20 cm, 30 cm and 40 cm.). By choosing different section lengths, the results differ substantially. The DAD-values for 10 cm distances strongly differs from DAD-values for 20 cm, 30 cm and 40 cm, because the result is strongly affected by the noise effect. For the measurement point distances of 30 cm and 40 cm, no significant changes become apparent. As in Fig. 18 shown, by considering the measurement point variation of 30 cm, the influence is reduced by up to 23,7%. The reduction of the influence from 30 cm to 40 cm amounts about 23,7–15,5 = 8,2%. Therefore, for the further

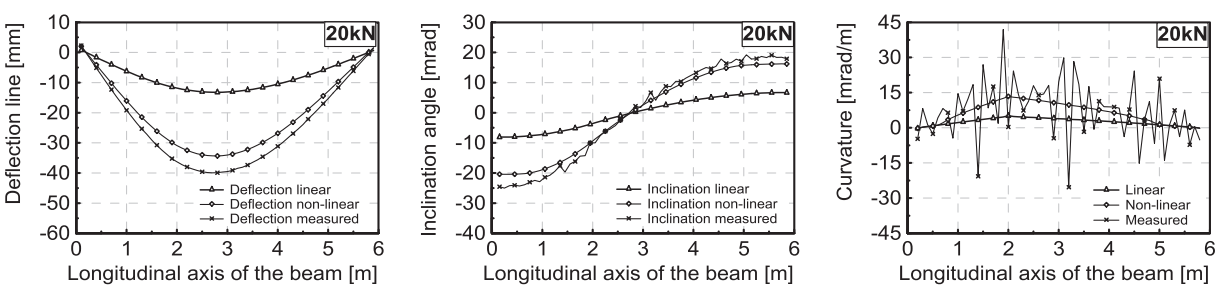

Fig. 14. Measured and calculated deflection lines, inclination angle and curvature for the load step 20 kN.

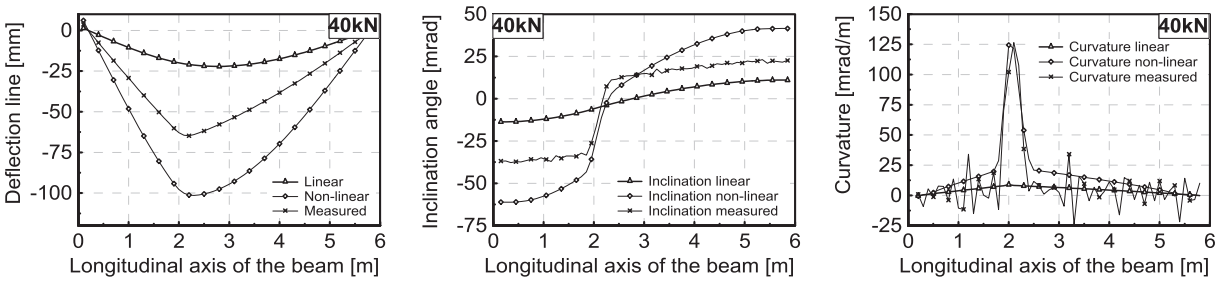

Fig. 15. Measured and calculated deflection lines, inclination angle and curvature for the load step 40 kN.

analysis and evaluation of the experiment the section length of 30 cm (every third measurement point) has been chosen as the on the other hand a close-range measurement grid increases the accuracy of damage localisation. Accordingly, the damage localisation accuracy is limited to 30 cm. A detailed description of the backgrounds and procedures has already been provided in Section 3.3.

4.4. Localisation of damage using DAD-method

As described in the experimental setup, each crack position and height is documented for each load step (part a. from Fig. 20 to Fig. 25). In this chapter, the localisation of the damage respectively local stiffness reduction due to cracking and concrete failure will be investigated. Thus, the DAD-values from curvature were calculated according to Eq. (6), which should highlight damage at discontinuities. Fig. 20 to Fig. 25 summarise the main results from the laboratory experiment. In part a. the documented cracks with their position and heights of the laboratory test are presented. Part b. shows the DAD-values for localisation of damage. The dash dotted lines in Part b. indicate the position of the supports and the dashed lines the beginning and ending of the cracked area. At load step 5,0 kN (Part a. Fig. 20), some cracks with low density have been detected. The DAD-values show for the same load step (Part b. Fig. 20) discontinuities in the same area with corresponding density. With load step 10 kN, the density increases as well as the cracked area (Fig. 20 to Fig. 24). The DAD-values from curvature show good accordance to the cracked area, which enables the localisation of the damage respectively area with the reduced stiffness. Fig. 25 also clearly shows the localisation of the concrete failure at about 2,0 m by the horizontal axis.

4.5. Case study: A steel beam experiment with local damages

The concept of damage detection for the case of crack formation in a concrete structure was shown in the previous chapters. Here, the loading of the beam was performed stepwise, whereby the width of the cracking area increased correspondingly. As measurement noise affects the accuracy of the method, more quantitative discussion on noise level and detectable damage severity is needed. Therefore, a laboratory test of a steel beam is presented and discussed (Fig. 26) in the following. In contrast to the reinforced concrete beam, the cross-section of the steel beam is stepwise damaged at three defined positions. The advantage of the steel beam is the fact that no additional cracking is to be expected outside the damage positions. The path-controlled load using a hydraulic press is carried out so that the maximum deflection does not exceed the serviceability limit state (22 mm). The span of the beam amounts to 5,60 m and the loading is applied at 2,00 m from the left end of the beam (Fig. 26). In total, three different damage positions are planned: damage position 1 at 3,60 m, damage position 2 at 4,80 m and damage position 3 at 1,20 m from the left side of the beam. The measurement of the deflection is also carried out using photogrammetry with reference points positioned at the steel supports and on the floor.

The damaging of the cross-section is applied by slitting the bottom flange of the HEA180 steel profile (Fig. 27). The paper includes the results of the experiment for four damage scenarios. Further results of the experiment with raw data without smoothing and the theoretical calculations can be found in [41]. Table 1 shows the degree of the damage which has been made manually at the three different positions by including the slit length within the flange and the deflection of the beam for the experimental load of 30 kN within the serviceability limit state. The slitting of the bottom flange is carried out gradually, symmetrically on both sides for each damage level (Fig. 27). For damage case 1/2, the degree of the stiffness reduction amounts to 5,2% and for damage case 1/4 and the degree of stiffness reduction was set to 23.8% at damage position 1 whereas the other two positions remain undamaged. Then for damage case 2/4, the degree of the damage at position 1 amounts to 49,0% and to 23,8% at position 2 whereas damage position 3 remains still undamaged. The last step 1/6 is subjected to a stiffness reduction of 71,5% at position 1 and 49,0% at the position 2 and 3. The slitting of the bottom flange is shown in Fig. 27.

The evaluation process of the test is similar as already presented in Section 4. The smoothing of the measured deflection line has been carried out within the standard deviation of the photogrammetry measurement. As measurement point variation, each third measurement point with 30 cm distances has been chosen (similar to Section 4.3).

Fig. 28 shows the results of damage detection using the DAD-values from curvature for the four damage scenarios. Fig. 28a. shows the DAD-values at a damage degree of 5,2% at position 1. Due to the noise effects

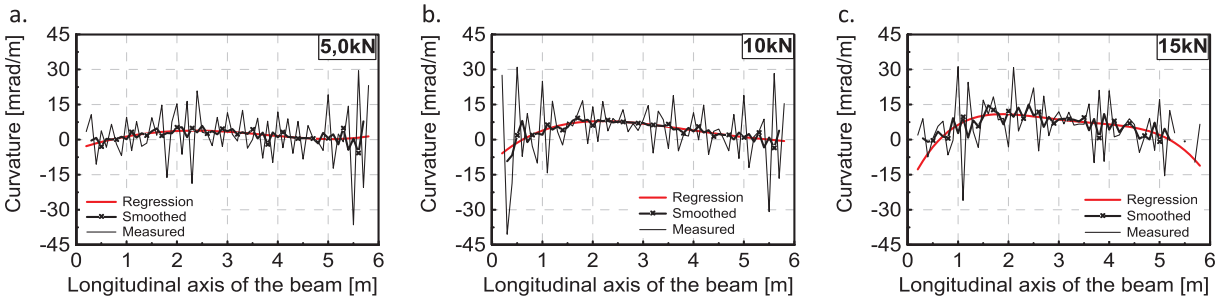

Fig. 16. Course of the curvature “red” from polynomial regression, “black with marker x” after smoothing and “black” from the raw measurement, A. load step 5 kN, B. 10 kN, C. 15 kN.

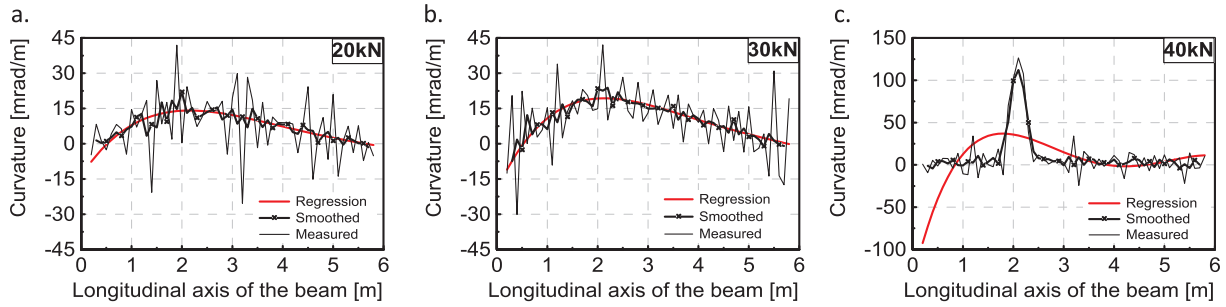

Fig. 17. Course of the curvature "red" from polynomial regression, "black with marker x" after smoothing and "black" from the raw measurement, a. load step 20 kN, b. 30 kN, c. 40 kN.

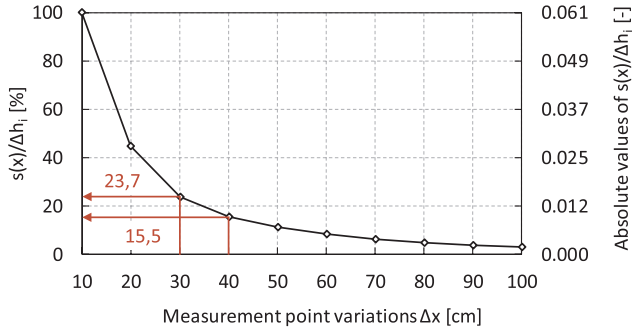

Fig. 18. Influence of the measurement point variation depending on the standard deviation.

resulting on the one hand from the measurement accuracy and on the other hand, from the path-controlled hydraulic press, a damage localisation was not possible for such a small stiffness reduction. There is only a range of DAD-values between 0,10 and 2,00 visible. In case of no existing damages, the DAD-values show peaks especially in the area with higher noise level. Thus, the range between 0,10 and 0,60 indicates bigger noise effect. At the damage degree of 23,8%, first discontinuities at the damage position become visible (Fig. 28b.), but there are still some peaks resulting from the noise effects outside of the range of the photogrammetry standard deviation. The peak at the left end is caused by the measurement noise (Fig. 28b.), which was already indicated in Fig. 28a. The clearly identification of the damage degree of 23,8% was not possible. However, the exact transition of the detectable degree of damage depending on the achieved measurement accuracy for this experiment lies in the range between 23,8% and 49,0%. In case of a stiffness reduction by about 49% (Fig. 28c.), the localisation of the damage was successfully achieved. The same diagram includes also the damage scenario at damage position 2 at damage degree of 23,8%. In case of two different damages, the larger one of the two could be clearly identified. The scaling of the vertical axis allows also the determination of damage level. Fig. 28d. shows the clear identification of the damage at position 1, even for the case where the loading and the damage position do not coincide. Fig. 29 shows the same diagram to the Fig. 28c and d, but the vertical axis is zoomed in order to detect the next discontinuity after the largest one. However, the small DAD-values were highly affected by noise and could not be clearly detected. The next chapter examines the noise and achieved accuracy of the experiment to discuss the optimisation potential of the method.

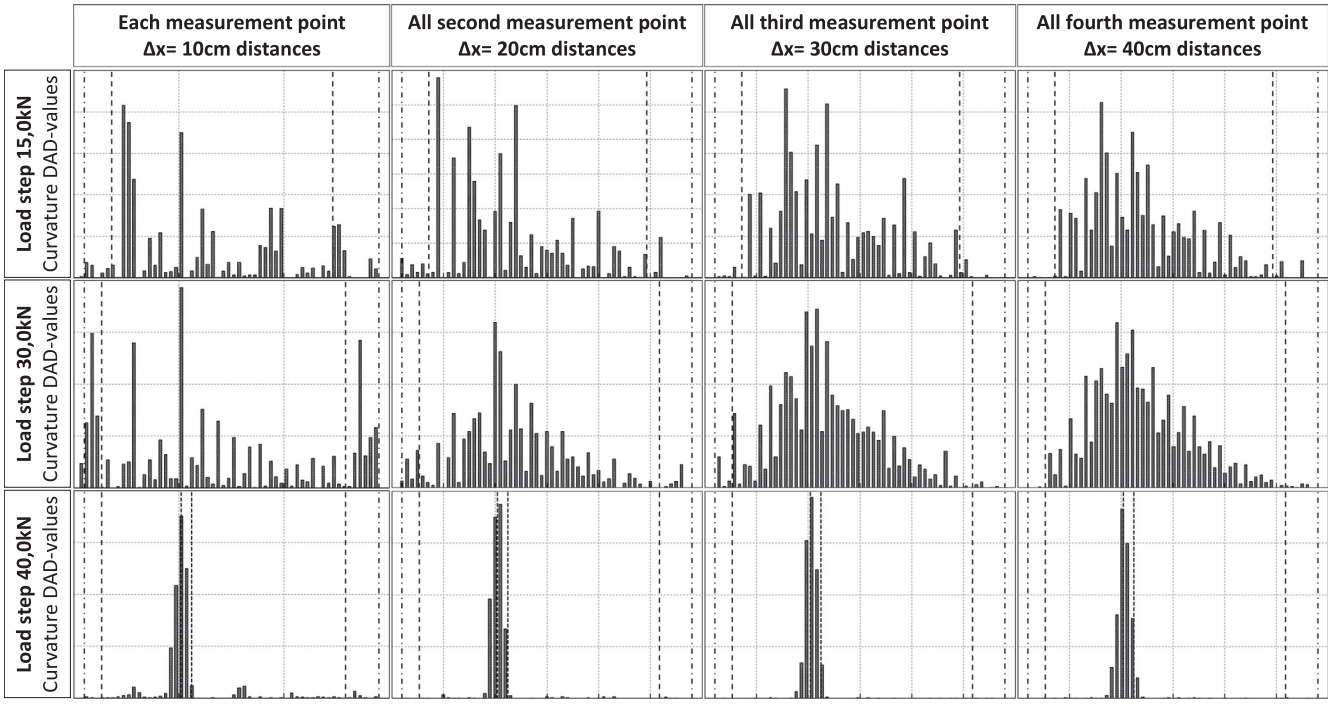

Fig. 19. Different variation of investigated section length exemplary for the load steps 15 kN, 30 kN and 40 kN.

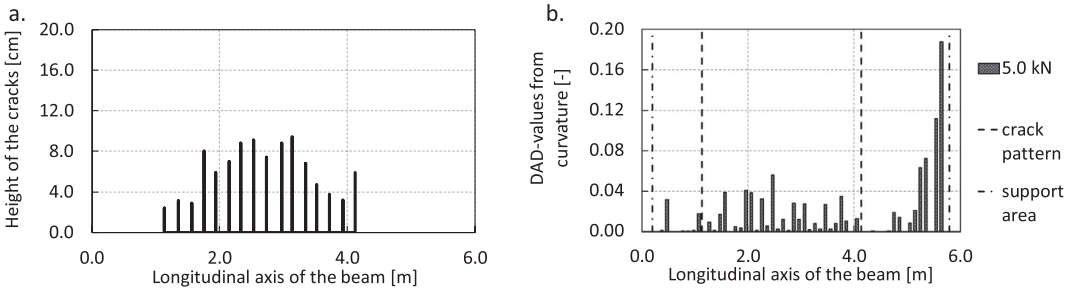

Fig. 20. a. Detected cracks in the experimental reinforced beam, b. DAD-values from curvature for load step 5,0 kN.

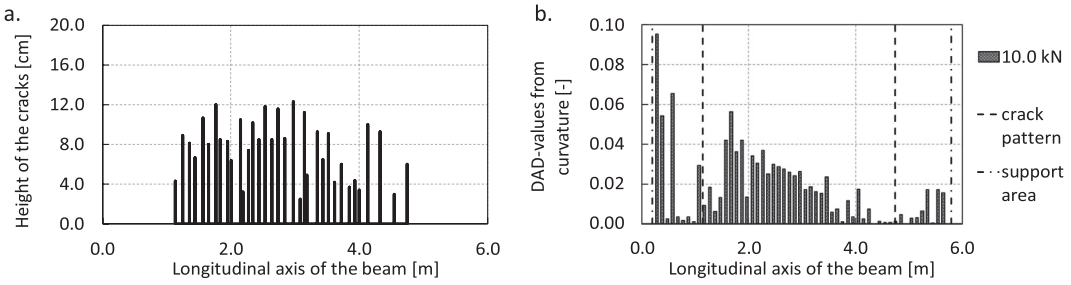

Fig. 21. a. Detected cracks in the experimental reinforced beam, b. DAD-values from curvature for load step 10 kN.

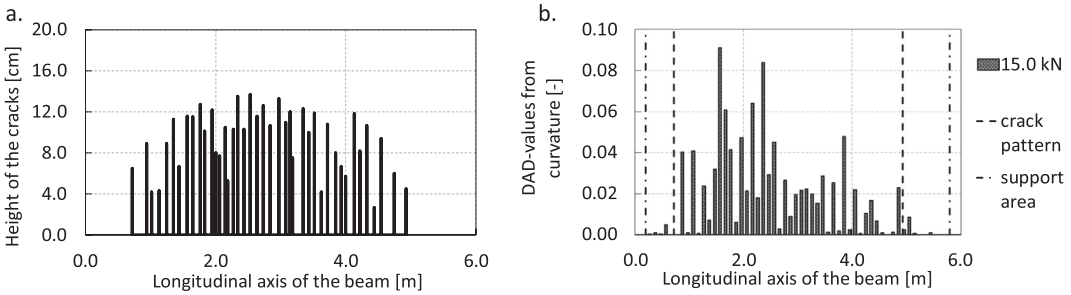

Fig. 22. a. Detected cracks in the experimental reinforced beam, b. DAD-values from curvature for load step 15 kN.

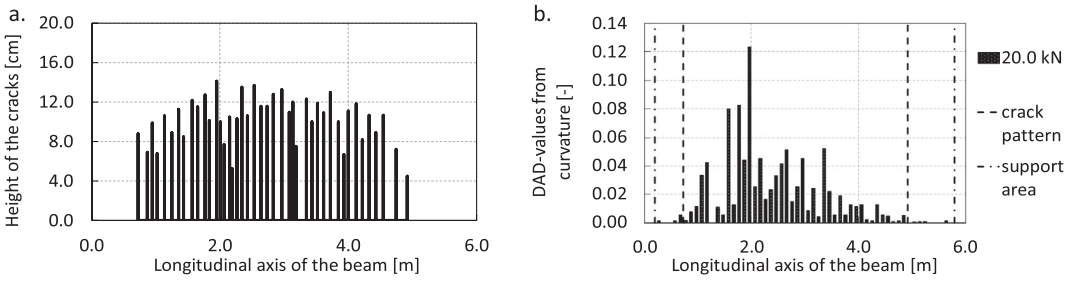

Fig. 23. a. Detected cracks in the experimental reinforced beam, b. DAD-values from curvature for load step 20 kN.

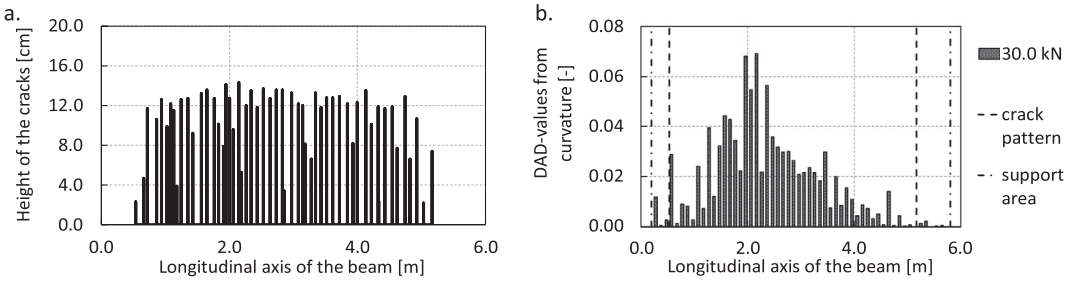

Fig. 24. a. Detected cracks in the experimental reinforced beam, b. DAD-values from curvature for load step 30 kN.

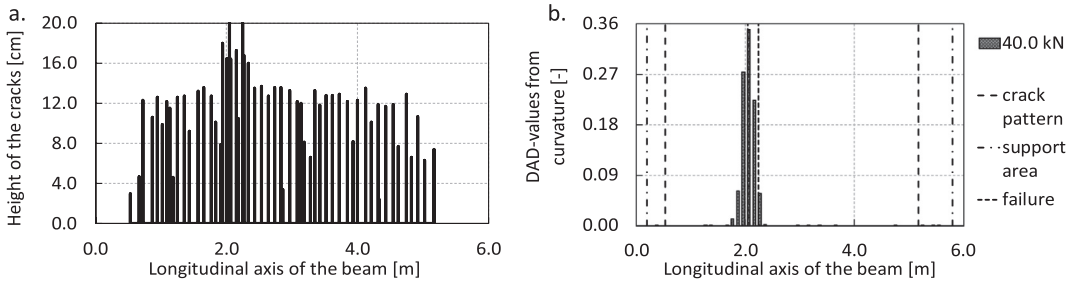

Fig. 25. a. Detected cracks in the experimental reinforced beam, b. DAD-values from curvature for load step 40 kN.

4.6. Analyse of the achieved accuracy and the noise effect

The DAD-method is used to localise damage in structures based on the measured deflection line. However, the accuracy of the deflection measurement is always affected by the applied technique. In this chapter, the noise level in the experiment will be discussed. Within the paper, two load deflection experiments with different damage scenarios and detection have already been presented. As already mentioned, the loading of both beam specimens are carried out by using a path-controlled hydraulic press. The hydraulic press is technically in very good condition and able to carry out the load very stably for several hours (Fig. 30). Nevertheless, the accuracy of the measurement results is influenced on one hand by the measurement technique and on the other hand by the vibration of the hydraulic. Fig. 30 shows a diagram for the loading process of the reinforced beam test. The vertical axis shows the deflection in millimetre and the horizontal axis the time in seconds. The measurement of the vertical deformation is done by using displacement sensors, which are positioned against the bottom surface of the concrete beam (Fig. 11). The diagram shows the deflection of the beam for the applied load steps 5,0 kN, 10 kN, 15 kN, 20 kN and 30 kN measured at 2,00 m from the left end of the beam, so at the position of the loading. In the following, the vibration of the beam under the load and without load is discussed to show the impact of the vibrations of the hydraulic press. The zoomed part A. in Fig. 30 shows the noise resulting from the hydraulic and from the displacement sensor, whereby the zoomed parts B and C present the noise only resulting from the displacement sensor. The difference between B.1 and B.2 is only the scale of the vertical axis. The parts A and B.1 as well as the parts B.2 and C are in the same scale. By analysing this data, a standard deviation of about 0,30 mm is found for part A and of about 0,01 mm for parts B and C. This means that although the deflection line was measured very precisely by photogrammetry (approx. 0,08 mm) and displacement sensors (0,01 mm), the total accuracy of the test was in the range of 0,30 mm. Nevertheless, the

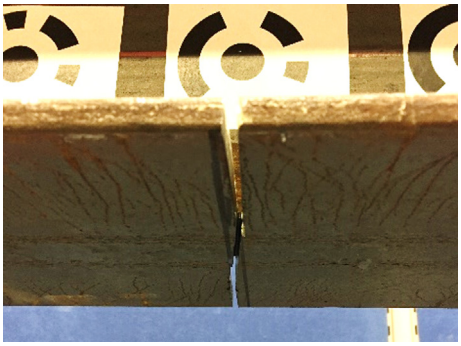

Fig. 27. Damaging of the cross-section by slitting the bottom flange.

DAD-method has shown that damages in the range between 23,8% and 49,0% or more can be localised based on the laboratory experiments. An experiment with static load (without hydraulic press) would significantly increase the sensitivity of the damage detection. This proves the high potential of the method.

4.7. Summary

Within the paper, the so-called Deformation Area Difference Method based on static load deflection experiments for identification and localisation of local damages is presented. The application of the DAD-method requires a very precisely measured deflection line of the structure obtained by a static load test as well as a theoretical model of the structure as reference. The method considers the area between the deflection lines, the inclination angles and the curvatures from both, the theoretical model as well as from the real measurement. The calculation of the inclination angle and curvature requires a multiple derivations of the deflection line. However, due to these the effect of

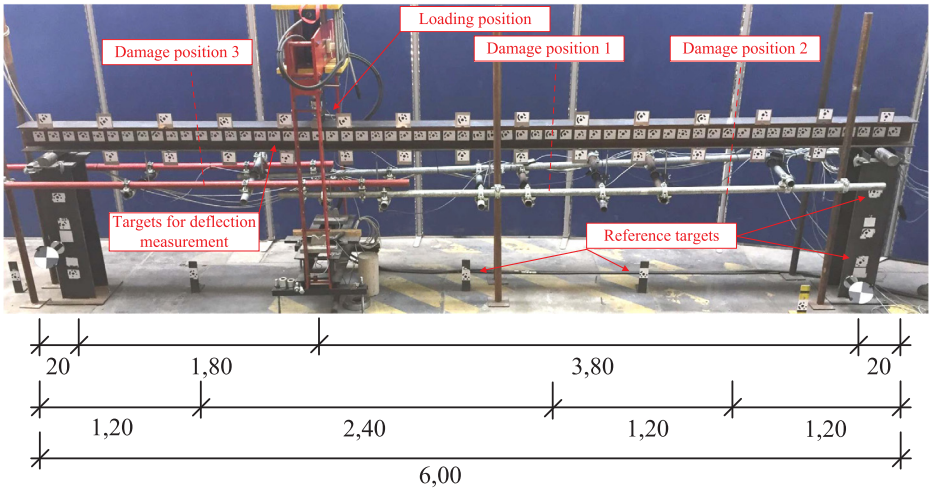

Fig. 26. Laboratory experiment with a steel beam and local damages.

Table 1
Damage levels and degree, deflection under 30 kN load.

Damage case	Damage degree [%]			Slit length within the flange [mm]	Deflection [mm]
	at position 1	at position 2	at position 3		
1/2	5,2	–	–	20	17,79
1/4	23,8	–	–	80	17,82
2/4	49,0	23,8	–	140 | 80	17,91
1/6	71,5	49,0	49,0	180 | 140 | 140	19,70

measurement noise is increased. The DAD-method considers the area between the curves, thus the function of the inclination angle and the curvature are again integrated, which leads again to a reduction of the noise effects. Naturally each measurement technique has a limited precision, even the photogrammetry.

The paper includes the description of the results from two laboratory experiments with a reinforced concrete beam and with a steel beam. The reinforced concrete beam is stepwise loaded until failure. The stepwise increase of the load leads to distinct crack patterns in the tensile zone, whereby the stiffness of the beam is reduced in this area. The aim of the study is to identify and localise the cracked area only by the information of the measured deflection line which has been measured by close-range photogrammetry. In contrast, the steel beam is loaded by 30 kN so that the serviceability limit state is not exceeded. The cross-section of the steel beam was gradually damaged at several positions. The aim of the study was to determine which degree of damage can be identified by the applied measurement technique and achieved accuracy. For this, a full-frame camera Nikon D800 is applied which is calibrated using a calibration wall with several targets. The targets of the calibration wall are measured by total station Leica TS30.

The key findings can be summarised as follows:

- The high precise measurement of the deflection line by using the technique of photogrammetry is enabled due to reference points (control points) and photogrammetric barcode targets. The calibration of the camera makes a significant contribution to the accuracy. Each measurement point is captured several times and delivers the coordinates of each point.
- Afterwards, a standard deviation for each measurement points is calculated. The reached accuracy respectively the standard deviation within the laboratory experiment amounts to about 0,07 mm.
- With the information of the standard deviation of photogrammetry, the measured deflection line is smoothed in order to reduce the noise effect and to identify with high probability discontinuities of the structure. The detected discontinuities out of the standard deviation for the photogrammetry are considered as a change in the stiffness or damage in the structure.
- Further investigations such as measurement point variability or polynomial regression as reference for the smoothing of the curve are included. The influence resulting from the measurement noise and the height difference between the measurement points is investigated in order to identify an optimum relation.
- An investigation of all accuracy influencing factors for the experiment is considered. Beside the measurement accuracy of photogrammetry, the loading process of the experimental beam using the path-controlled hydraulic had an influence for the total accuracy of the test. Despite the total standard deviation, it was possible to identify the damage.
- In case of several local damages in a structure, first only the biggest damage can be identified. Although, the detection of the next smaller damage can be done based on theoretical results, the presented experimental results could not show this. This will need further investigations.
- The investigation of the steel beam has shown that the sensitivity of

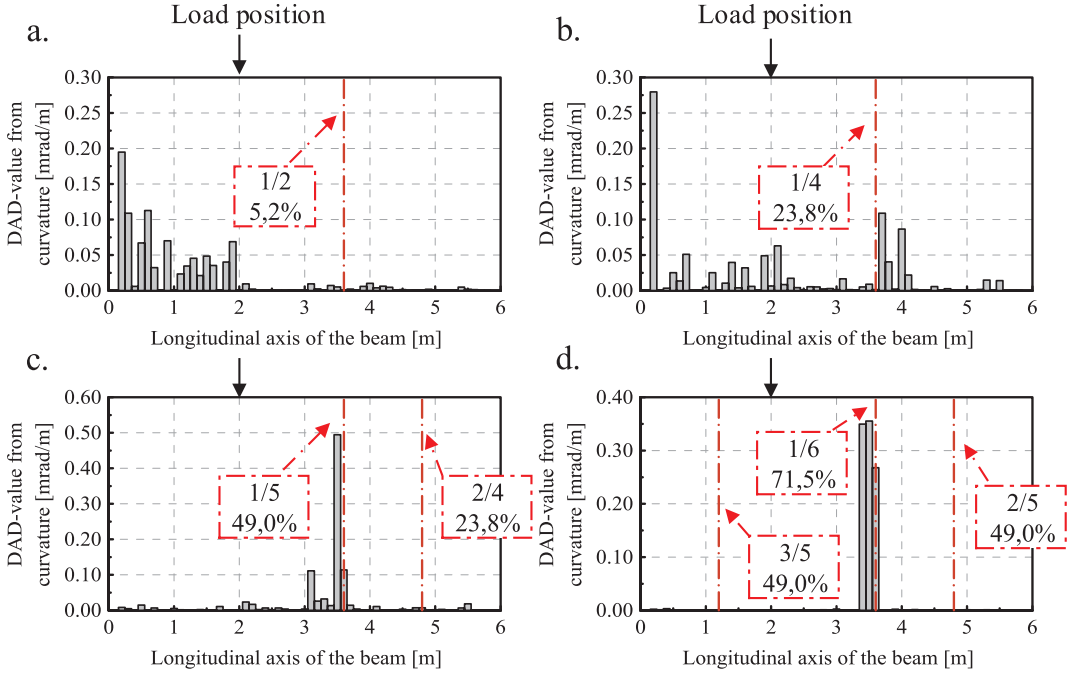

Fig. 28. DAD-values from curvature a. damage position 1, damage level 2, damage degree 5,2%; b. damage position 1, damage level 4, damage degree 23,8%; c. damage position 2, damage level 4, damage degree 23,8%, d. damage position 1.

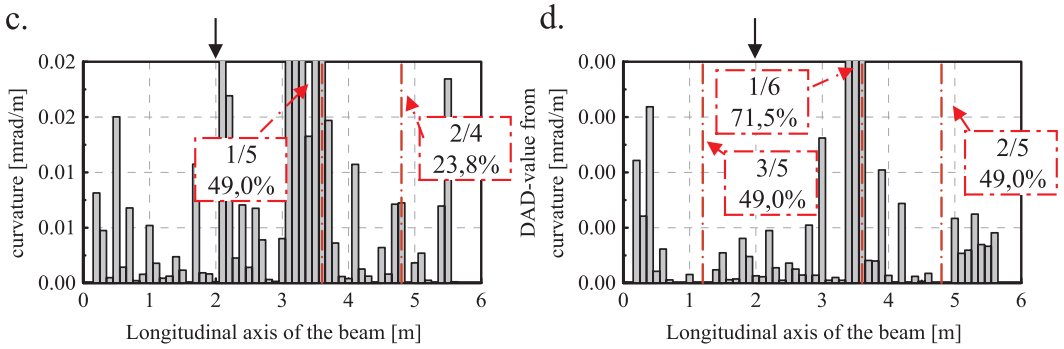

Fig. 29. Zoom of the vertical axis of Fig. 28c and d.

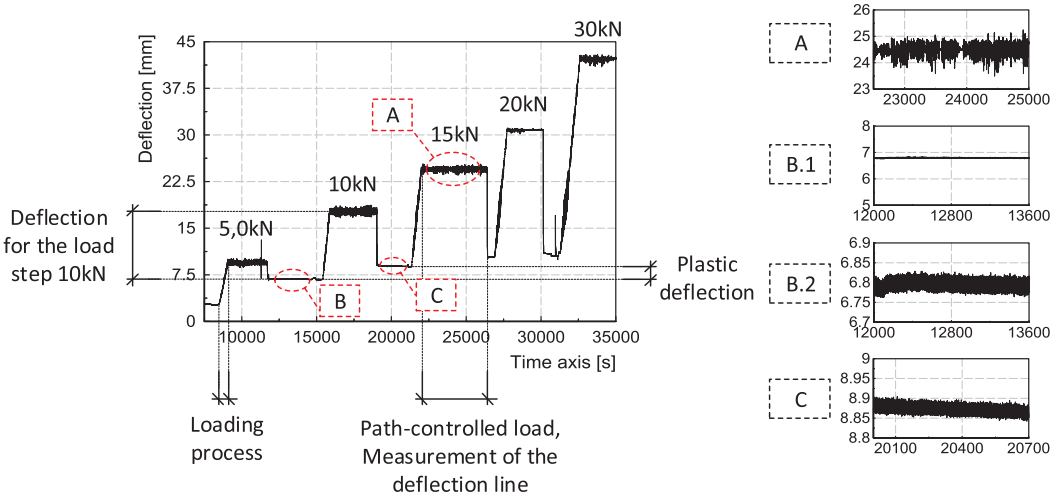

Fig. 30. The noise effect for the reinforced concrete beam experiment.

the method depends on the damage intensity and the achievable accuracy of the measurement technique. In the presented test, the achieved accuracy of the photogrammetry with the standard deviation of 0,06 to 0,11 mm was able to detect local stiffness reductions of about in the range between 23,8% and 49,0% or more. In general, the accuracy of photogrammetry could still be improved and reach standard deviation values of only 0,01 to 0,03 mm with the help of camera enhancement systems and an optimization of the calibration process. The total accuracy of the test could be significantly improved due to stable respectively static load. Therefore, there is still room to improve the sensitivity of damage detection using the DAD-method. During the first laboratory experiment, each crack in the concrete is documented and integrated to graphs. The comparison of the crack pattern with the course of the DAD-values shows good correlation. Even within the serviceability limit state of the beam with small deflections the DAD-method allowed the localisation of the cracked area. The second laboratory experiment with a steel beam proved that the method is also able to detect local damages. The steel beam was only slightly deformed so that the maximum deflection did not exceed the serviceability limit state. However, within the experiment, the noise resulting from the hydraulic press was technically not controllable and increased noise effects. For this reason the authors suggest that the loading for the next experiment should take place using a static load, which should improve the sensitivity of the method allowing the localisation of smaller damage.

The DAD-method shows considerable potential for the future for damage assessment from the combination of intelligent algorithms and innovative measurement techniques.

References

[1] Ferrari P. The effect of the competition between cars and trucks on the evolution of the motorway transport system. Transp Res Part C May 2009;17:558–70.
[2] Commission E. The EU explained: Transport. Luxembourg: Publications Office of the European Union; 2014.
[3] P. Croney and D. Croney, The Design and Performance of Road Pavements, 1994.
[4] Niggemann M. Angewandter Straßenbau. Hameln: Springer Vieweg; 2012.
[5] Scheer J. Failed Bridges: Case Studies, Causes and Consequences. Hannover: Wilhelm Ernst & Sohn; 2010.
[6] B. f. S. (bast), "http://www.bast.de" [Online]. Available: http://www.bast.de/DE/Statistik/statistik-node.html [Accessed 11 10 2017].
[7] Davis, S.L., Goldberg, D. "The Fix We're In For: The State of Our Nation's Bridges 2013," Transportation for America, 2013.
[8] Brunell G, Kim YJ. Effect of local damage on the bevavior of a laboratory-scale stees truss bridge. Eng Struct 2013;48:281–91.
[9] Döhler M, Hille F, Mevel L, Rücker W. Structural health monitoring with statical methods during progressive damage test of S101 bridge. Eng Struct 2014;69:183–93.
[10] Bolle G, Schacht G, Marx S. "Loading tests of existing concrete structures - historical development and present practise", in *fib Symposium PRAGUE*. Czech Republic 2011.
[11] Comisu C-C, Taranu N, Boaca G, Scutaru M-C. Structural health monitoring system of bridges. Procedia Eng 2017;199:2054–9.
[12] Kaplan V, Dvorak P. Reflection on the possibilities for monitoring the aging bridge structures. Procedia Eng 2017;187:649–55.
[13] Kotes P, Brodnan M, Ivaskova M, Dubala K. Influence of reinforcement corrosion on shear resistance of RC bridge girder subjected to shear. Procedia Eng 2015;111:444–9.
[14] Helmi K, Taylor T, Zarafshan A, Ansari F. Reference free method for real time monitoring of bidge deflections. Eng Struct 2015;103:116–24.
[15] Lantsoght EO, Veen Cvd, Boer Ad, Hordijk DA. State-of-the-art on load testing of concrete bridges. Eng Struct 2017;150:231–41.
[16] Stöhr, S., Link, M., Rohrmann, R., Rücker, W. "Damage detection based on static measurements on bridge structures," in IMAC-XXIV, USA. 2006.
[17] Zhang W, Sun LM, Sun SW. Bridge-deflection estimation through inclinometer data considering structural damages. J Bridge Eng February 2017;22(2).
[18] Koleková Y, Kovác M, Baláz I. Influence lines of bridges with box-girder cross-section under torsion and distorsion. Procedia Eng 2017;190:603–10.

[19] Sun Z, Nagayama T, Fujino Y. Minimizing noise effect in curvature-based damage detection. J Civil Struct Health Monitor April 2016;6:255–64.
[20] He W-Y, Ren W-X, Zhu S. Damage detection of beam structures using quasi-static moving load induced displacement responce. Eng Struct May 2017;145:70–82.
[21] He W-Y, Ren W-X, Zhu S. Baseline-free damage localization method for statically determinate beam structures using dual-type response induced by quasi-static moving load. J Sound Vib April 2017;400:58–70.
[22] Zhang W, Li J, Hao H, Ma H. Damage detection in bridge structures under moving loads with phase trajectory change of multi-type vibration measurements. Mech Syst Sig Process 2017;87:410–25.
[23] Cavadas F, Smith IF, Figueiras J. Damage detection using data-driven methods applied to moving-load responses. Mech Syst Sig Process September 2013;39(1–2):409–25.
[24] Li J, Hao H. Damage detection of shear connectors under moving loads with relative displacement measurements. Mech Syst Sig Process August 2015;60–61:124–50.
[25] Nguyen KV. Comparison studies of open and breathing crack detections of a beam-like bridge subjected to a moving vehicle. Eng Struct March 2013;51:306–14.
[26] Carr AJ, Jáuregui DV, Reveiro B, Arias P, Armesto J. Structural evaluation of historic masonry arch bridges based on first hinge formation. Cunstr Build Mater 2013;47:569–78.
[27] Baqersad J, Poozesh P, Niezrecki C, Avitabile P. Photogrammetry and optical methods in structural dynamics - A review. Mech Syst Sig Process February 2017;86:17–34.
[28] Lee H, Rhee H. 3-D measurement of structural vibration using digital close-range photogrammetry. Sens Actuators, A March 2013;196:63–9.
[29] Arias P, Armesto J, Di-Capua D, González-Drigo R, Lorenzo H, Pérez-Gracia V. Digital photogrammetry, GPR and computational analysis of structural damages in a mediaeval bridge. Eng Fail Anal 2007;14:1444–57.
[30] Jiang R, Jáuregui DV, White KR. Close-range photogrammetry applications in bridge measurement: Literature review. Measurement 2008;41:823–34.
[31] Jiang R, Jauregui DV. Development of a digital close-range photogrammetric bridge deflection measurement system. Measurement 2010;43:1431–8.
[32] Nishiyama S, Minakata N, Kikuchi T, Yano T. Improved digital photogrammetry technique for crack monitoring. Adv Eng Inf 2015;29:851–8.
[33] Riveiro B, González-Jorge H, Varela M, Jáuregui DV. Validation of terrestrial laser scanning and photogrammetry techniques for the measurement of vertical under-clearance and beam geometry in structural inspection of bridges. Measurement 2013;46(1):784–94.
[34] Capéran P, Poljansek M, Gutiérrez E, Primi S, Paulotto C. Optical 3-dimensional measurements on a FRP beam tested at serviceability limit. Compos Struct 2012;94:3465–77.
[35] Erdenebat D, Wadmann D, Scherbaum F, Teferle FN. The Deformation Area Difference (DAD) method for condition assessment of reinforced structures. Eng Struct 2018;155:315–29.
[36] Erdenebat, D. Waldmann, D. “Condition assessment and damage localisation for bridges by use of the Deformation Area Difference Method (DAD-Method),” in fib Symposium, Cape Town, 2016.
[37] Erdenebat, D., Waldmann, D., Teferle, F.N. “Numerical investigations of bridges with the aim of condition assessment in applying the Deformation Area Difference method (DAD-method) and selecting appropriate measurement techniques,” in IALCCE, Delft, 2016.
[38] Erdenebat D, Waldmann D, Teferle FN. “Laboratory experiment for damage assessment using the DAD-method”, in Fourth Conference on Smart Monitoring. Zürich: Assessment and Rehabilitation of Civil Structures; 2017.
[39] Marciukaitis G, Juknevicius L. Deviation in deflections of eccentrically prestressed reinforced concrete structures. Procedia Eng 2017;172:706–10.
[40] Patel BN, Sivakumar DP, Srinivasan M. A simplified moment-curvature based approach for large deflection analysis of micro-beams using the consistent couple stress theory. Eur J Mech A/Solids 2017;66:45–54.
[41] D. Erdenebat, D. Waldmann and F. N. Teferle, “Static load deflection experiment on a beam for damage detection using the Deformation Area Difference Method,” in IALCCE2018, Ghent, 2018.